

MONITORING TEMPERATURE PATTERNS AT SELECTED WORLD HERITAGE SITES IN EGYPT USING HIGH RESOLUTION WORLDCLIM DATA

VIRANCH N.DAVE*

Department of Geography, The Maharaja Sayajirao University of Baroda, Vadodara, Gujarat, India

*Email: viranch.n-geogphd@msubaroda.ac.in

Received 28 August 2023, accepted in revised form 9 October 2023



Abstract

Climate change is considered a major challenge to World Heritage Sites, be they natural or cultural. Monitoring long-term temperature patterns helps in assessing changes in the climatic conditions of an area. In this study, trend analysis of mean temperature patterns at the selected World Heritage Sites in Egypt is done using parametric and non parametric methods. Parametric simple linear regression is used to derive the slope and R square value, while non-parametric methods such as the Mann-Kendall method and Sen's slope estimate are used to derive the trend and magnitude of mean temperature values. The data requirement for the study is fulfilled using gridded maximum and minimum temperatures from WorldClim. The calculation of the mean temperature is done using QGIS. Analysis of results for the whole period (1960-2021) reveals a positive trend for all Sites. However, results for the first half (1960-1990) show no significant trend at most Sites except Abu Simbel and Abu Mena. The second half of the whole period (1991-2021) showed a significant positive trend for all the Sites, with higher magnitudes being observed for Sites located in lower Egypt and the Sinai Peninsula. This study can serve as the foundation upon which detailed longitudinal site specific investigation can be made.

Keywords: heritage, climate change, trend analysis, linear Regression, Mann-Kendall method, Sen's Slope estimate, temperature

1. Introduction

It becomes necessary to comprehend long term temperature patterns in order to get proper clarity regarding the changes that are taking place. According to Berkeley Earth estimates, the earth has already warmed by 1.3° celsius compared to pre-industrial levels (Berkeley Earth, 2023) and this has already resulted in a substantial rise in the occurrence of 'extreme weather events' like

droughts, heatwaves, wildfires, cyclones, and others (Khatib, 2023). Global warming has almost negatively affected the lives of people (Malakouti, 2023). Warming temperatures have serious interlinked consequences ranging from compromising food security to a rise in the sea level, changes in the rate of precipitation, an increase in the salinity of both surface and ground water, and so on (Rezvi et al., 2023). The focus on monitoring the risk of climate change on cultural

heritage has started receiving significant attention after the publication of the sixth assessment report of the IPCC (Ismael et al., 2023). The sixth assessment report noted the widespread impact of climate change on cultural heritage, which results in increasing vulnerability to adaptive capacity and creating losses in the sense of belonging, valued cultural practices, identity, and so on (Lee et al., 2023). Over the last few decades, it has also been realized that World Heritage Sites (which include both natural and cultural heritage) are incessantly exposed to the changes in the climatic parameters that are taking place (Vyshkvarkova & Sukhonos, 2023). UNESCO has identified the changes in temperature, wind intensity, and so on as significant causes of concern for World Heritage Sites (Sesana et al., 2021).

Over the last five decades, there has been a significant increase in temperature observed over the African continent (Engelbrecht et al., 2015). Cultural heritage Sites on the African continent are at greater risk from these environmental fluxes, and they are not prepared and adapted to future climatic hazards (Pörtner et al., 2022). Evidence from carbon-14 (C14) dating indicates that the Saharan region (of which Egypt is a part) started a shift towards drier climatic conditions before 6100 years ago (Adams & Faure, 1997). Therefore, it can certainly be deduced that all the important heritage Sites of Egyptian civilization have been exposed to these drier and more arid climatic conditions since the time they were made. Since the last few years, scholars have directed their attention towards studying the temperature trends in Egypt. In 2020, the temperature increased to 1.8°C in Egypt above pre-industrial levels (Berkeley Earth, 2023), which is 0.5°C higher than the world average. Studies have proved that climatic change is quite well pronounced in Egypt, and the temperatures are rising rapidly in areas with intense human activity (Hereher, 2016). The impact of global atmospheric pressure systems on the distribution of temperature conditions over Egypt helps in understanding

the spatial variability; thus, the normal trend indicates that the temperature increases from north to south (Eid et al., 2019). Studies have found from air temperature data derived from different meteorological stations in Egypt that the air temperature in Egypt is three times higher than the global temperature (Domroes & El-Tantawi, 2005, as cited in Hereher, 2016).

The stones of which the monuments in Egypt are made must have gone through weathering and disintegration owing to their exposure to the outside atmosphere (Ismael, 2015). However, the process of natural weathering is slow but there are studies which shed light on the fact that changes in climatic conditions can exacerbate the disintegration of monuments (Camuffo, 1986; Sabbioni et al., 2008; Sabbioni et al., 2010; Brimblecombe et al., 2011; Ismael, 2015). Several experts have noticed discoloration and cracking being witnessed at the monuments of Luxor and the Great Pyramids in Memphis, along with others, due to the changes in temperature and humidity (Farouk, 2019). Exposure of stones to ultraviolet (UV) radiation may also result in their discoloration (Sitzia et al., 2021). In the south, near Aswan, the ancient monuments, which are built up of granite rock, are suffering from a scathing temperature rise. A study conducted by Ismael et al. (2023) on the historical temples and fortresses of Kharga Oasis in Egypt provides evidence for the erosion rates due to changes in temperature, wind, and precipitation rates.

Of late, there have been works that have focused on providing mitigation measures for heritage properties that are exposed to climate change. Blavier et al. (2023) comprehensively mention the direct and indirect impacts of temperature, moisture, precipitation, wind, and solar radiation on heritage buildings while also providing adaptive solutions. A study conducted by Becherini et al. (2016) evaluated the performance of shelters that were added to the UNESCO World Heritage Site of the Megalithic Temples of Hagar Qim and Mnajdra

located in Malta to protect from changes in air temperature and humidity conditions. The changing climatic parameters may influence the natural World Heritage Site in a different way. The site of Wadi Al Hitan in Egypt, which is known for its geotourism potential due to the presence of fossilized remains, is also covered with shelters to protect them from getting exposed to unstable temperatures and humidity, which can result in deterioration (Newsome et al., 2012).

The focus of the present study is not to provide any recommendations related to mitigation and adaptation strategies for the World Heritage Sites that are exposed to climate change. The main focus of this study is on monitoring changes in mean temperature patterns for some selected World Heritage Sites in Egypt for the period 1960–2021 using WorldClim 2.1 data. Monitoring is a continuous process; it helps in understanding the changes in the climatic parameters that are witnessed at heritage Sites, and therefore it eventually forms the basis for adaptive management (Cave, 2022). Worldclim uses weather station data to provide high resolution interpolated gridded climate data using thin plate splines with different covariates like elevation, distance from the coast, land surface temperature, and cloud cover that give highly accurate temperature data (Fick & Hijmans, 2017). The main reason behind the reliance on high resolution grid based datasets in this study is that most of the meteorological stations in Egypt are located in the vicinity of the Nile Valley and its delta, which are prominent urban areas constituting only five to six percent of the country's total geographical area, thus resulting in an uneven distribution of climatic data (Hereher, 2016). Secondly, such gridded datasets are interpolated using different authentic datasets derived from meteorological stations and satellite based remote sensing. It gives the best estimates of different climatic variables for those locations that are situated far away from meteorological stations (Haylock et al., 2008). So far, seven properties have been designated

as World Heritage Sites in Egypt by UNESCO. The details pertaining to these sites are given in Table 1. Of these seven properties, Wadi-Al-Hitan is the only one that belongs to the natural category, while all others are cultural properties. Some properties are associated with multiple locations, like the Nubian monuments that have ten different locations; Ancient Thebes and its Necropolis are associated with three locations; Memphis and its Necropolis include two locations; and Historic Cairo further north in Egypt includes five locations.

2. Materials and Methodology

Site selection and Data collection

In order to analyze the temporal variations in mean temperature at the World Heritage properties in Egypt, certain Sites were selected. Three World Heritage properties (Wadi al Hitan, Abu Mena, and St. Catherine) have only one location each, so these three Sites were automatically selected for this study. The remaining four properties (the Nubian monuments- from Abu Simbel to Philae; the Ancient Thebes and its Necropolis; the Memphis and its Necropolis; and the Historic Cairo) are associated with multiple locations (Table 1). Considering factors like the size of the World Heritage property and the temperature variations between the multiple locations, only one location is chosen from each World Heritage property that has multiple locations.

The World Heritage property of the Nubian Monuments- from Abu Simbel to Philae, consists of ten locations covering a large geographic area from 22° 20' 14"N to 24° 04' 39.7"; therefore, only the Abu Simbel temple is selected in this study. For the remaining World Heritage properties having multiple locations, like the Ancient Thebes and its Necropolis, the Memphis and its Necropolis, and the Historic Cairo, there were no temperature variations observed between the multiple locations of each of these three properties. Therefore, in this study, Ancient

Table 1. UNESCO World Heritage Sites in Egypt

World Heritage Property	Multiple locations (if any)	Lat.	Long.
	Abu Simbel	22° 20' 14"	31° 37' 32.9"
	Amada	22° 43' 52.1"	32° 15' 45.4"
	Wadi Sebua	22° 47' 35.5"	32° 32' 43.3"
	Kalabsha	23° 57' 39.16"	32° 52' 01.02"
Nubian Monuments from Abu Simbel to Philae	Philae (Island of Agilkia)	24° 01' 30.64"	32° 53' 04.67"
	Old and Middle Kingdom Tombs	24° 06' 10.8"	32° 53' 24.9"
	Ruins of town of Elephantine	24° 05' 04.6"	32° 53' 09.4"
	Stone quarries and obelisk	24° 04' 37"	32° 53' 43.5"
	Monastery of St. Simeon	24° 05' 41"	32° 52' 33.3"
	Islamic Cemetery	24° 04' 39.7"	32° 53' 29.5"
Ancient Thebes & its Necropolis	Temple of Luxor	25° 41' 59.5"	32° 38' 20.5"
	Temple of Karnak	25° 43' 08"	32° 39' 26.1"
	Ancient Thebes Necropolis	25° 43' 53.2"	32° 35' 49.3"
Wadi al Hitán		29°19'59.99"	30°10'59.99"
Memphis and its Necropolis- The Pyramid fields from Giza to Dashur	Site of Memphis	29° 51' 19.8"	31 15 39.8
	Pyramid fields from Giza to Dahshur	29°58'33.74"	31° 7'49.48"
Historic Cairo	Al-Fustat	30° 00' 24"	31° 14' 00.4"
	Mosque of Ahmed Ibn Tulun, The Citadel Area, The Fatimid Nucleus of Cairo, Necropolis	30° 02' 39.9"	31° 15' 43.7"
	Al-Imam ash-Shaf'i Necropolis	30° 00' 38"	31° 15' 28.5"
	As-Sayyidah Nafisah Necropolis	30° 01' 17.5"	31° 15' 27.4"
	Qayitbay Necropolis	30° 02' 49.6"	31° 16' 37.1"
Abu Mena		30°50'9.00"	29°40'0.00"
St Catherine		28°33'22.43"	33°58'31.55"

Source- Information derived from UNESCO (<https://whc.unesco.org/en/statesparties/eg>)

Note: Sites in bold letters are selected in this study.

Thebes is selected from the three locations of Ancient Thebes and its Necropolis, while the Site of Memphis is selected from Memphis and its Necropolis, and the mosque of Ahmad Ibn Tulun is selected from the five locations of Historic Cairo. The selected Sites are shown on the map (Figure 1). This map is prepared in QGIS 3.20.2 using the geographic coordinates (latitude/longitude) of these Sites, that were derived from UNESCO World Heritage convention website (<https://whc.unesco.org/en/statesparties/eg>).

After getting the coordinates for the

locations selected in this study, Google Earth software is used to download the coordinates in Keyhole Markup Language (KML) file format. Temperature data is derived from WorldClim 2.1 (Fick & Hijmans, 2017). WorldClim provides gridded data for multiple atmospheric parameters, like rainfall and temperature, from 1960 to 2021. WorldClim data is downscaled from CRU-TS 4.06 (Harris et al., 2020). Minimum and maximum temperature data from the years 1960 to 2021 is being downloaded with a spatial resolution of 2.5 minutes.

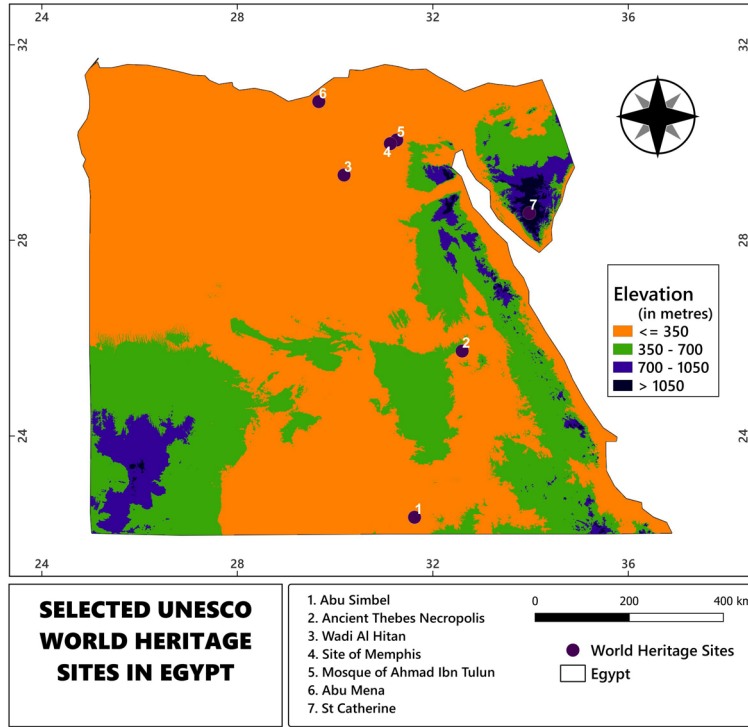


Fig. 1. Showing the location of selected world heritage Sites in Egypt

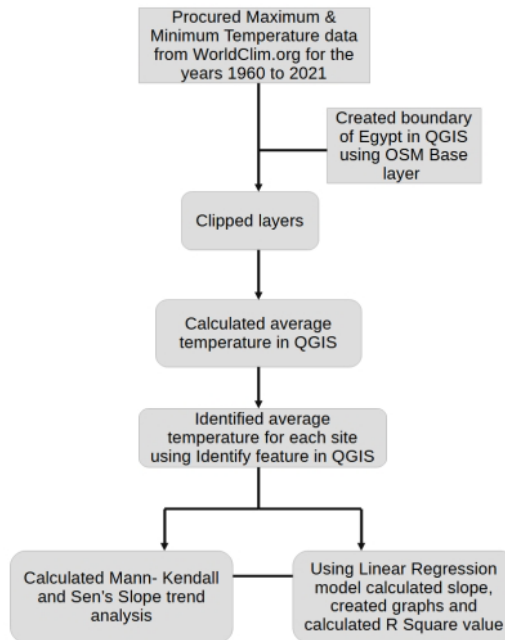


Fig. 2. Methodology chart

Data Processing and Analysis

The downloaded WorldClim data is available month-wise in GeoTiff format. For calculating the mean temperature, the GeoTiff files for both minimum and maximum temperature data are downloaded. The Geotiff files for both minimum and maximum temperature are available separately in WorldClim. Thus, for each month, a separate layer of minimum and maximum temperature is available, and for the entire year, a combination of 24 layers for minimum and maximum temperature (12 each). Therefore, for the entire period of study from 1960 to 2021 (62 years), a total of 1488 layers (744 for maximum and 744 for minimum temperature) were used and opened in QGIS 3.20.2 to calculate the mean average temperature using the r.series tool. Further on, the boundary of the Arab Republic of Egypt (created using the OSM base layer in QGIS) was used to extract the study area from the Geo Tiff layers, which are for the entire world. The coordinates of the selected World Heritage Sites, which were downloaded in KML, were then overlaid on this average temperature layer. Finally, the year-wise average temperature for the selected World Heritage Sites was derived using an Identify feature tool in QGIS environment (Figure 2).

A 30-year normal period is defined as the 'Climatological Baseline Period' by the World Meteorological Organization (WMO) (James J. MacCarthy et al., 2001). According to the IPCC report (Masson-Delmotte et al., 2018), global warming is defined as an increase in the 30-year averaged global surface air and sea surface temperature. This paper attempts to demonstrate the trends of the mean temperature values for the selected World Heritage Sites in Egypt over the period 1960–2021. Moreover, the mean temperature values for the first (1960-1990) and second (1991-2021) half of the whole period are compared to get an idea of how the trend behaved from 1960–1990 and 1991–2021. As Climatologists usually calculate new averages for every 30 years (NOAA, 2019),

in this study, the entire 62-year time period is divided into two equal halves of 31 years each, hence the temperature patterns are analyzed for the three temporal periods, from 1960 to 2021, from 1960 to 1990, and from 1991 to 2021.

Trend analysis is done using the ordinary least squares approach of the simple linear regression model for understanding temperature patterns at each site. Using simple linear regression, the relationship between temperature and time or year is identified. This relationship is shown by creating a scatter plot and calculating the coefficient of determination (R square) value in LibreOffice Writer. The trend and magnitude of the average annual temperature at each World Heritage site are also being analyzed using the Mann-Kendall (MK) test and Sen's slope estimate (SSE). These calculations are being done using the 'Non-Parametric Trend Tests and Change Point Detection' package in R Studio software.

Linear regression analysis is a parametric test as it requires some form of a priori knowledge regarding the functional relationship (Mahmoud, 2019). On the other hand, both the Mann-Kendall test and Sen's slope estimate are non parametric tests, which require data to be independent in contrast to parametric tests, which necessitate data to be independent and also to be normally distributed (Gocic & Trajkovic, 2013). Taking climate change into account, there are a number of studies that have used Mann-Kendall and Sen's slope methods to determine the existence of significant trends in hydro-meteorological data such as temperature, precipitation, and so on (Yue & Wang, 2002).

The simple linear regression model involves one dependent variable Y and one independent variable X, where any changes in X result in a change in Y (Chervenkov & Slavov, 2019). The following equation;

$$y=ax+b \quad (1)$$

Where Y is the dependent variable, X is the independent variable, and a and b are the

slope and intercept. In this study, slope ‘a’ indicates the increase or decrease in mean temperature in degrees Celsius (°C). Positive ‘a’ values indicate an increase, while negative ‘a’ shows a decrease in mean temperature.

Statistically Mann-Kendall test for any time series data X_1, \dots, X_n uses the following statistics (Mohammad et al., 2022).

$$S = \sum_{i=1}^{n-1} \sum_{j=i+1}^n \text{sign}(T_j - T_i) \tag{2}$$

$$\text{Where sign}(T_j - T_i) = \begin{cases} 1 & \text{if } (x_j - x_i) > 0 \\ 0 & \text{if } (x_j - x_i) = 0 \\ -1 & \text{if } (x_j - x_i) < 0 \end{cases} \tag{3}$$

x_j and x_i represent data values at times j and i , respectively.

Variance (S) is computed as

$$\text{Var}(S) = \frac{n(n-1)(2n+5) - \sum_{i=1}^m t_i(t_i-1)(2t_i+5)}{18} \tag{4}$$

(where n is the number of data points, m is the number of tied groups, whereas t_i denotes number of ties up to sample i)

If the sample size is $n > 10$ then Z_{mk} statistic is computed as (Gocic & Trajkovic, 2013).

$$Z_{mk} = \begin{cases} \frac{S-1}{\sqrt{\text{var}(S)}}, & \text{if } S > 0 \\ 0, & \text{if } S = 0 \\ \frac{S+1}{\sqrt{\text{var}(S)}}, & \text{if } S < 0 \end{cases} \tag{5}$$

The results derived give Z_{mk} and P values (probability values). If the value of Z_{mk} is positive, then the value shows an increasing trend; conversely, if the value of Z_{mk} is negative, then the trend is decreasing in nature (Curiac & Micea, 2022; Jain & Bhatt, 2022). This Z_{mk} value helps in evaluating the presence or absence of a statistically significant trend in the data. If the derived Z_{mk} value is greater than $Z_{1-\alpha/2}$ (where the Z value is obtained from the standard normal table or z table and the α is the significance level), the null hypothesis is rejected (Kandya et al., 2021). Now, the rejection of the null hypothesis means that there is some significant trend in the data, while accepting

the null hypothesis certainly indicates no significant trend (Agbo & Ekpo, 2021). In this study, different significance levels ($\alpha = 0.05$ and 0.01) were applied.

Sen’s slope estimate is extensively used to identify the magnitude of trends in meteorological data (Rahman et al., 2022). Assuming the trend to be linear, Sen’s slope estimate is used (Thenmozhi & Kottiswaran, 2016).

$$f(t) = Qt + B \tag{6}$$

In the above equation (6), $f(t)$ is a function of time, representing a time series that can be increasing or decreasing; Q is the slope; B is a constant; and t is time.

Sen’s slope equation for N pair of data is written as follows:

$$Q_i = \frac{x_j - x_i}{j - i} \tag{7}$$

Here Q_i is the slope magnitude per year (Jiqin et al., 2023). If $j > i$, then N values are calculated as follows:

$$N = n(n-1)/2 \tag{8}$$

Where N indicates the number of calculated slopes, while n is the number of data points.

The Mann-Kendall provides statistical significance and also shows the direction in which it is increasing or decreasing, while Sen’s slope estimate gives information regarding the magnitude of the trend (Raju, 2021).

3. Results and Discussion

In this section, systematic analysis and discussion are being done on mean temperature trends at the World Heritage Sites in Egypt using parametric and non-parametric methods. Efforts are being made to identify the behavior of mean temperature at all the selected World Heritage Sites for the period 1960 to 2021; moreover, attempts are being made to analyze and present the results of mean temperature by dividing the overall period (1960 to 2021) into two sub-periods: from 1960 to 1990 and from 1991 to

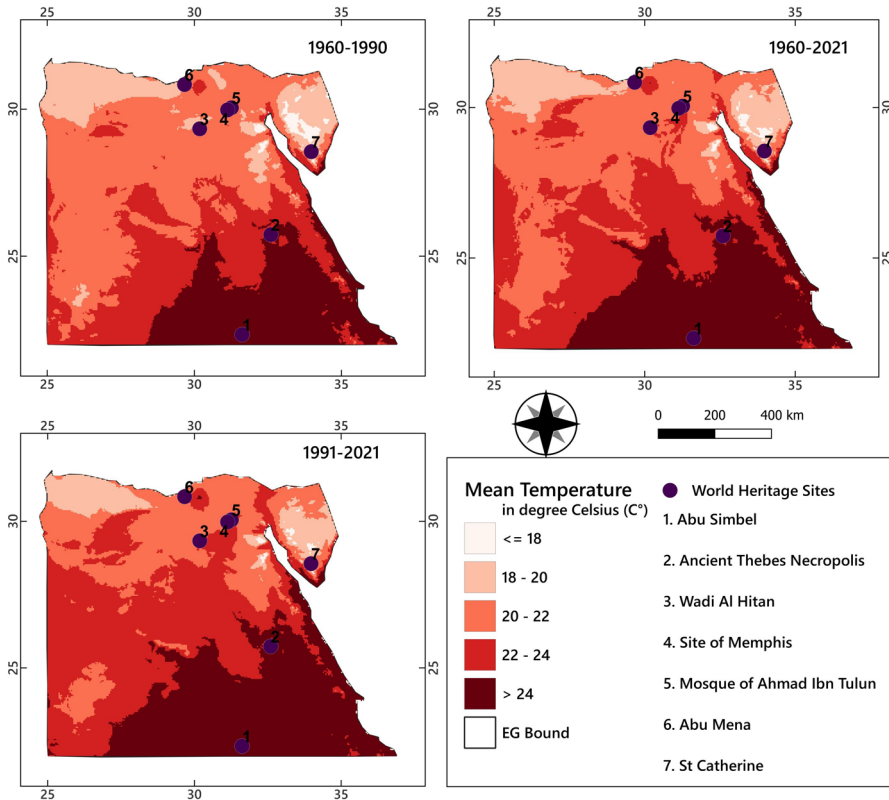


Fig. 3. Showing the location of selected world heritage Sites in Egypt

2021. Maps showing the distribution of mean temperature values in Egypt for the first and second half and the whole period are shown in Figure. 3. Results are presented in tabular and graphic form.

Temperature Trends for selected Sites from 1960 to 2021

This subsection presents the results for the mean temperature trends that were being observed at the selected World Heritage Sites in Egypt for the period 1960 to 2021, which covers the entire period of this study. Figure 4 shows the graphical representation of mean annual temperature for all the Sites for the period 1960 to 2021.

The highest mean temperature reported during this period is for Abu Simbel (26.42°C), while the lowest is being observed at St. Catherine (16.92°C). The mean temperature values for Ancient Thebes Necropolis

(25.11°C), Wadi Al Hitan (21.76°C), Site of Memphis (22.1°C), Mosque of Ahmad Ibn Tulun (22.18°C), and Abu Mena (20.83°C) are being noted moving north from Abu Simbel (Table.2). The slope of the regression equation clearly demonstrates that the trend is in an increasing direction for all the Sites at the 99% confidence level (Table 2). The positive slope 'a' values indicate that the mean temperature is found to be increasing for every site during the period 1960–2021. The increase in mean temperature during this period is found to be highest at Abu Simbel (0.033°C/year) and lowest at Abu Mena (0.022°C/year). For other Sites that are located on the mainland of Egypt between Abu Simbel in the south and Abu Mena in the north, the mean temperatures reported are as follows: Ancient Thebes Necropolis (0.027°C/year), Wadi Al Hitan (0.0241°C/year), Site of Memphis (0.0242 °C/year), and the Mosque of Ahmad Ibn Tulun (0.023°C/

Table 2. Mean temperature values derived using parametric and non parametric methods (1960-2021)

Name of the site	Fundamental Statistics		Linear regression			Mann-Kendall and Sen's Slope		
	Mean	Standard deviation	a	b	t statistic	R ²	Z _{mk}	Q
Abu Simbel	26.42	0.74	0.033	39.76	10.45**	0.64	7.37**	0.036
Ancient Thebes Necropolis	25.11	0.69	0.027	29.95	8.02**	0.51	6.56**	0.030
Wadi Al Hitan	21.76	0.6	0.0241	26.39	8.11**	0.52	6.11**	0.025
Site of Memphis	22.1	0.64	0.0242	26.25	7.19**	0.46	5.52**	0.025
Mosque of Ahmad Ibn Tulun	22.18	0.64	0.023	25.40	6.93**	0.44	5.32**	0.025
Abu Mena	20.83	0.62	0.022	24.48	6.77**	0.43	4.98**	0.023
St Catherine	16.92	0.7	0.025	34.61	8.57**	0.43	5.19**	0.027

**Level of significance 0.01

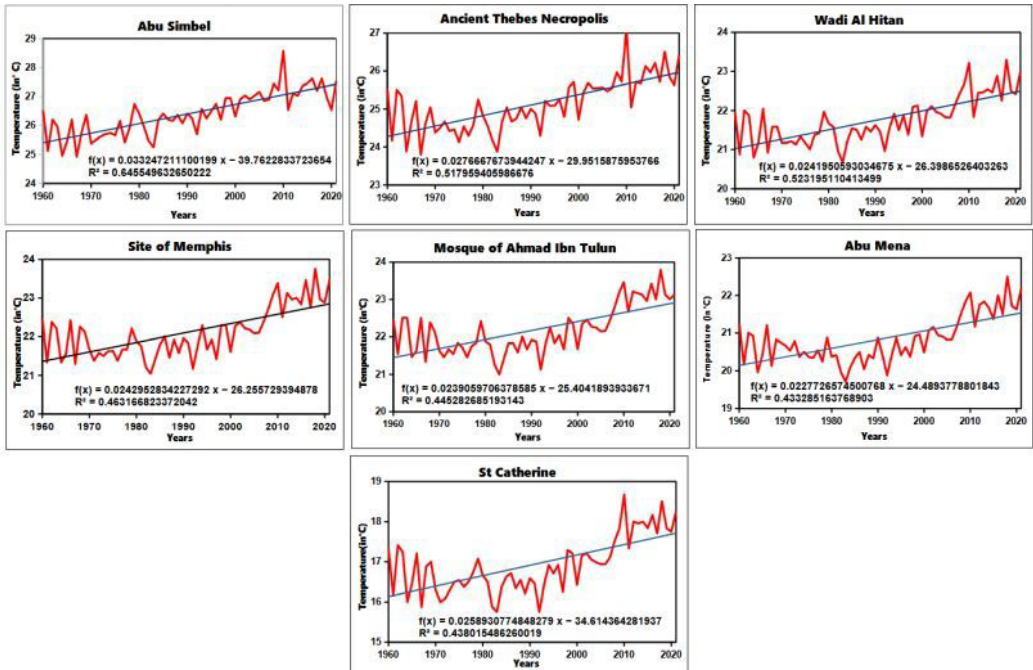


Fig. 4. Trends of average annual temperature for selected World Heritage Sites in Egypt from 1960 to 2021

year). The mean temperature of 0.025°C per year is observed for St. Catherine, which is located on the Sinai Peninsula.

The graphs (Figure.4) also shows the coefficient of determination value (R-square). It is being observed that the R square value is the lowest for St. Catherine (0.43). On

the mainland of Egypt, Abu Simbel has the highest R square value (0.64), while Abu Mena has the lowest R square value (0.43). The R square value for Ancient Thebes Necropolis (0.51) is lower compared to that of Abu Simbel, which is located south of Ancient Thebes Necropolis. Moving

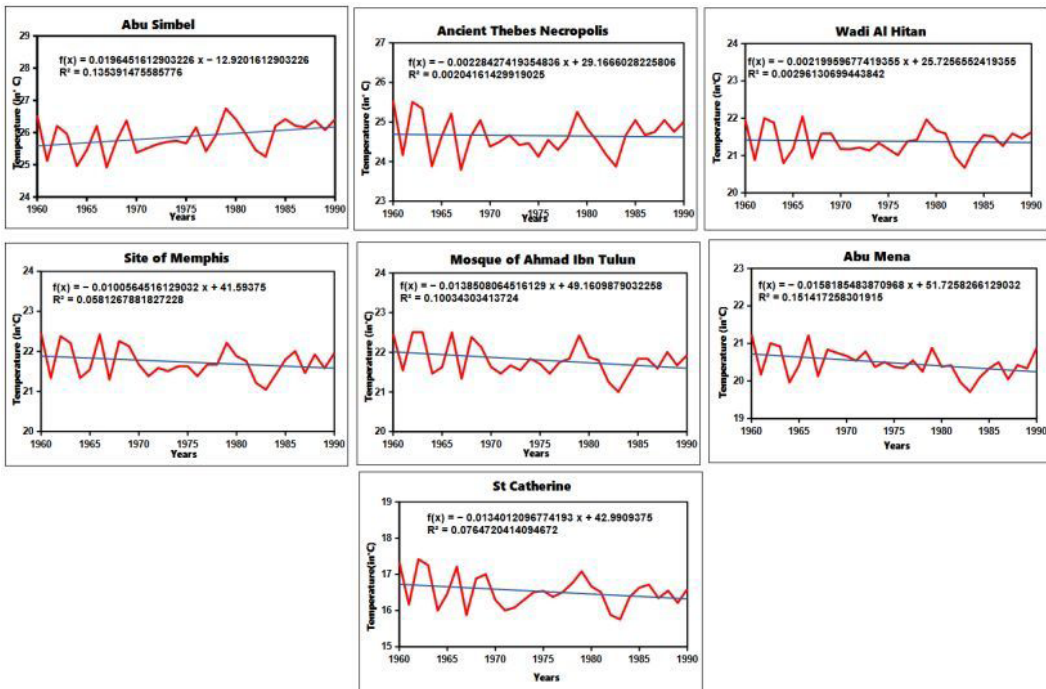


Fig. 5. Trends of average annual temperature for the selected World Heritage Sites in Egypt for (1960-1990)

north of the Ancient Thebes Necropolis, the R square for the site of Wadi Al Hitan (0.52) is slightly higher. However, further north to Wadi Al Hitan, the R Square keeps getting lower, such as at the Site of Memphis (0.46) and the Mosque of Ahmad Ibn Tulun (0.44). The value of R square (which shows how much the variations in the dependent variable are explained by the variations in the independent variable) is observed to be decreasing from south to north, with the exception of Wadi Al Hitan during this period.

The Z_{mk} values derived using the Mann-Kendall test for all the Sites are found to be statistically significant at 99% confidence. The positive Z_{mk} values show an upward trend in mean temperature for all Sites. The value of Sen's slope, demonstrating the magnitude of the trend, indicates that the mean temperature increased by $0.036^{\circ}\text{C}/\text{year}$ for the site of Abu Simbel, which is the highest value observed among all the Sites. Apart from Abu Simbel, the Sites located on mainland Egypt that recorded an annual hike in mean temperature are the Ancient Thebes

Necropolis ($0.030^{\circ}\text{C}/\text{year}$), Wadi Al Hitan ($0.025^{\circ}\text{C}/\text{year}$), Site of Memphis ($0.025^{\circ}\text{C}/\text{year}$), Mosque of Ahmad Ibn Tulun ($0.025^{\circ}\text{C}/\text{year}$), and Abu Mena ($0.023^{\circ}\text{C}/\text{year}$). St. Catherine on the Sinai Peninsula witnessed an annual increase of 0.027°C per year.

Temperature trends for the selected Sites from 1960 to 1990

Results and discussion pertaining to the mean temperature for all the selected World Heritage Sites in Egypt for the period 1960–1990 have been presented in this subsection. Figure 5 shows the graphical representation of mean temperature in relation to time or years for all the Sites.

The mean temperature values reported during this phase for all selected Sites show that the highest is for Abu Simbel (25.88°C), while the lowest is noted for St. Catherine (16.52°C). In between these, Sites like the Ancient Thebes Necropolis (24.65°C), Wadi Al Hitan (21.38°C), the Site of Memphis (21.73°C), the Mosque of Ahmad Ibn Tulun

Table 3. Mean temperature values derived using parametric and non parametric methods 1960-1990

Name of the site	Fundamental Statistics		Linear regression				Mann-Kendall and Sen's Slope	
	Mean value	Standard Deviation	a	b	t statistic	R ²	Z _{mk}	Q
Abu Simbel	25.88	0.48	0.019	12.92	2.13*	0.13	1.99*	0.027
Ancient Thebes Necropolis	24.65	0.46	-0.0022	29.16	-0.24	0.002	0.30	0.003
Wadi Al Hitan	21.38	0.37	-0.0029	25.72	-0.29	0.002	0.39	0.002
Site of Memphis	21.73	0.38	-0.010	41.59	-1.33	0.058	-0.44	-0.005
Mosque of Ahmad Ibn Tulun	21.8	0.4	-0.013	49.16	-1.79	0.10	-0.78	-0.005
Abu Mena	20.48	0.37	-0.015	51.72	-2.27*	0.15	-2.21*	-0.025
St Catherine	16.52	0.44	-0.013	42.99	-1.54	0.07	-0.78	-0.020

*Level of significance 0.05

(21.8°C), and Abu Mena (20.48°C) are all located on the mainland of Egypt (Table.3). During this phase, the study reported a positive slope 'a' value for the site of Abu Simbel (0.019 °C/year), while for all the other Sites, slope 'a' values were found to be negative. However, the slope values are statistically significant at 95% confidence intervals only for Abu Simbel and Abu Mena. For Abu Mena, the value of 'a' observed is -0.015 °C/year. The coefficient of determination value is highest at Abu Mena (0.15), followed by Abu Simbel Temple (0.13), Historic Cairo (0.10), St. Catherine (0.07), Site of Memphis (0.05), Wadi al Hitan (0.0029), and Ancient Thebes (0.0020). In this case, very few variations in the dependent variable (temperature) are explained by the independent variable (time or year).

The Z_{mk} values derived by using the Mann-Kendall test show that except at Abu Simbel and Abu Mena, the trend is found to be statistically insignificant. Abu Simbel shows an upward trend with Sen's slope magnitude value of 0.027°C/year, while at Abu Mena, Sen's slope magnitude of -0.005°C/year shows a downward trend. Sen's slope values are also found to be negative for the Site of Memphis (-0.005°C/year), the Mosque of Ahmad Ibn Tulun (-0.005°C/year), and St. Catherine (-0.020°C/year); however, they are

not statistically significant based on their Z_{mk} values. Sites that have positive Sen's slope values but do not have statistically significant Z_{mk} are Ancient Thebes Necropolis (0.003°C/year) and Wadi Al Hitan (0.002°C/year).

Temperature trends for the selected Sites from 1991 to 2021

In this subsection, the mean temperature trends from 1991 to 2021 are being analyzed. The mean temperature recorded during this period shows that the highest value is observed for Abu Simbel (26.95 °C), and conversely, the lowest is being reported for St. Catherine (17.32°C). The mean temperature values for Ancient Thebes Necropolis (25.58°C), Wadi Al Hitan (22.14°C), Site of Memphis (22.47°C), Mosque of Ahmad Ibn Tulun (22.55°C), and Abu Mena (21.19°C) were reported during this period. Figure 6 demonstrates the graphical representation of the mean temperature for the selected World Heritage Sites for the period 1991-2021.

Table 4 shows that the slope 'a' values for all the Sites are positive, therefore, the increasing trend for the mean temperature is observed. The slope values are found to be statistically significant at the 99% confidence level. Slope 'a' is found to be highest for St. Catherine (0.064°C/year), while the lowest value is found for Abu Simbel (0.038°C/year).

Table 4. Mean temperature values derived using parametric and non parametric methods (1991-2021)

Name of the site	Fundamental Statistics		Linear regression			Mann-Kendall and Sen's Slope		
	Mean	Standard Deviation	a	b	t statistic	R ²	Z _{mk}	Q
Abu Simbel	26.95	0.55	0.038	49.98	4.43**	0.40	4.16**	0.039
Ancient Thebes Necropolis	25.58	0.57	0.044	62.70	5.35**	0.49	4.55**	0.04
Wadi Al Hitan	22.14	0.55	0.048	75.34	7.12**	0.63	4.69**	0.046
Site of Memphis	22.47	0.64	0.060	98.90	8.87**	0.73	5.00**	0.059
Mosque of Ahmad Ibn Tulun	22.55	0.63	0.059	97.67	9.10**	0.74	4.81**	0.057
Abu Mena	21.19	0.63	0.060	100.01	9.71**	0.76	5.28**	0.06
St Catherine	17.32	0.69	0.064	112.72	8.57**	0.71	5.05**	0.062

**Level of significance 0.01

On the Egyptian mainland, the slope values reported for other Sites such as the Ancient Thebes Necropolis (0.044°C/year), Wadi Al Hitan (0.048°C/year), the Site of Memphis (0.060°C/year), the Mosque of Ahmad Ibn Tulun (0.059°C/year), and Abu Mena (0.060°C/year) show an increasing trend. The coefficient of determination is found

to be highest for Abu Mena (0.76), while the lowest is observed for Abu Simbel (0.40). In this period, the R Square noted for other Sites like Ancient Thebes (0.49), Wadi al Hitan (0.63), Site of Memphis (0.73), Historic Cairo (0.74), and St. Catherine (0.71) shows that the variations in the dependent variable (average temperature) can be explained by

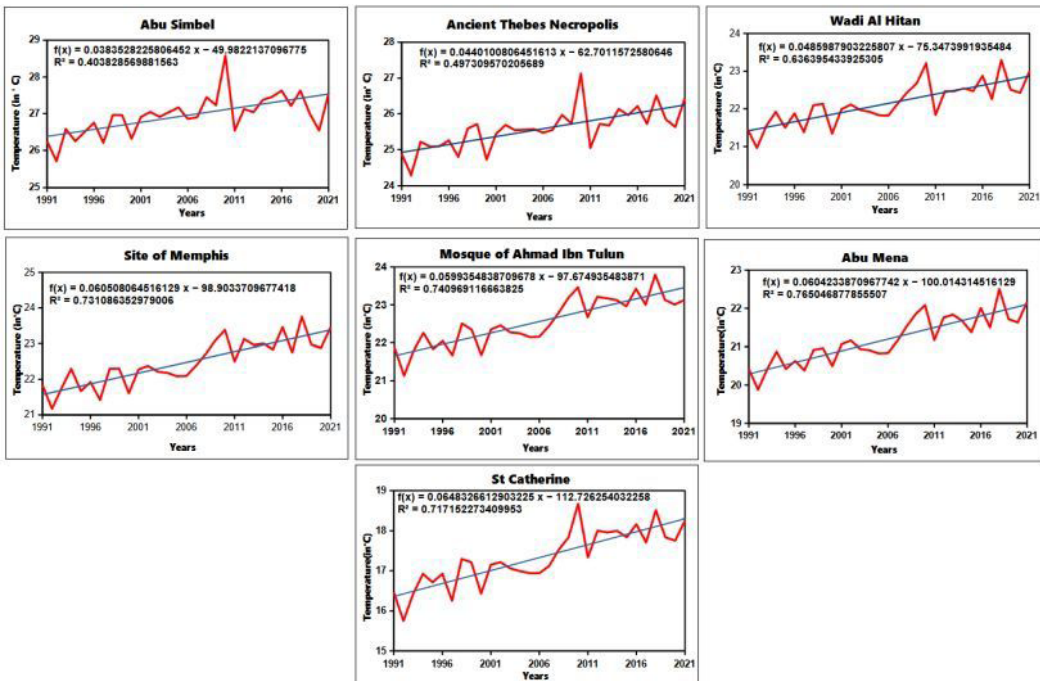


Fig. 6. Trend of average annual temperature for the selected World Heritage Sites in Egypt (1991-2021)

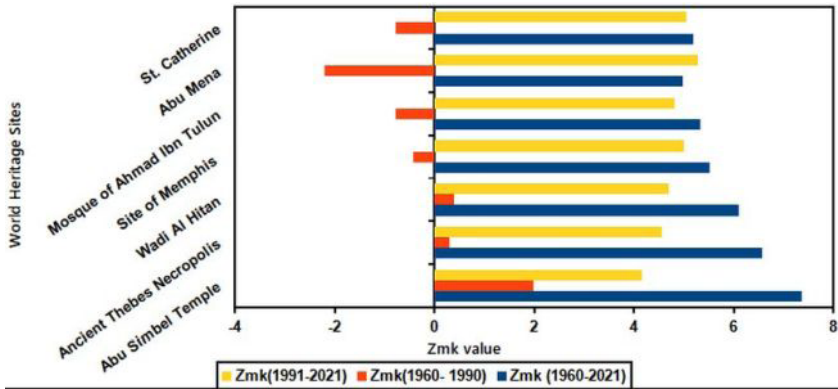


Fig. 7. Z_{mk} values for the selected world heritage Sites in Egypt at different time phases

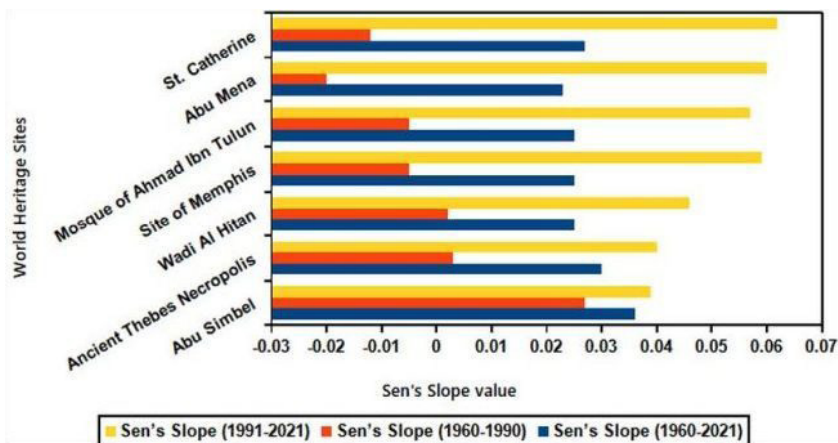


Fig. 8. Sen's slope values for the selected world heritage Sites in Egypt at different time phases

the independent variable (year/time).

Mann-Kendall and Sen's slope values observed during the period 1991–2021 for the selected World Heritage Sites are presented graphically in Figure 7 and 8 and also shown in tabular form in Table 4. The Z_{mk} values given in Table 4 for all Sites show an increasing trend at a 99% confidence level. The Sen's Slope magnitude values for the Sites on the mainland from south to north are: Abu Simbel (0.039°C/year), Ancient Thebes (0.04°C/year), Wadi al Hitan (0.046°C/year), Site of Memphis (0.059°C/year), the Mosque of Ahmad Ibn Tulun (0.057°C/year), and Abu Mena (0.06°C/year). St. Catherine on Sinai Peninsula recorded the highest Sen's Slope value of 0.062°C/year.

Key drivers

Historically, the mainland of Egypt has witnessed a general latitudinal north-south gradient in temperature patterns. Conversely, in this study, the mean temperature values for the selected World Heritage Sites are less influenced by the latitudinal gradient, and the slight variations show that there are some exceptions to it. Moreover, the slope values derived using linear regression and Sen's slope estimate for the period 1991–2021 are higher for the Sites located in north Egypt compared to those in south Egypt. The site on the Sinai Peninsula reported the highest Sen's slope and slope of linear regression from 1991 to 2021. This clearly points out that there are multiple drivers behind the spatio-temporal temperature variations

observed for the World Heritage Sites in Egypt. The mean temperature at Sites like Abu Simbel and Ancient Thebes Necropolis that are located in upper Egypt follows the latitudinal gradient for the three periods being analyzed; however, the slope values are higher for Ancient Thebes Necropolis during the period 1991–2021 compared to Abu Simbel. Progressing north from the Ancient Thebes Necropolis, the mean temperature of the three Sites 'Wadi Al Hitan, the Site of Memphis, and the Mosque of Ahmad Ibn Tulun' shows that they are less influenced by latitudinal variations. Many heritage Sites in Egypt are already facing environmental problems due to the increase in urban areas and the rapid rise in population (Elfadaly et al., 2023). The tangible heritage, particularly those that are located in urban areas, is at risk of climate change due to the many different pressures that are acting upon it (Sardella et al., 2020). In Egypt, it is observed that those places that are located away from urban areas do record comparatively less temperature than those locations that are situated closer to urban areas, as urban places are associated with considerable anthropogenic activities (Hereher, 2016).

The results derived in this study show that the site of Wadi Al Hitan, which is located south of the Site of Memphis, has lower mean temperature values. This can be due to the fact that Wadi Al Hitan is located away from urban areas and closer to the Western Desert. The Mosque of Ahmad Ibn Tulun, which is located north of the Site of Memphis, has higher mean temperature values compared to later. It is being observed that the release of greenhouse gases like carbon dioxide (CO₂), methane (CH₄), and nitrous oxide (N₂O) due to the burning of rice straw has led to the absorption and re-emission of the outgoing longwave terrestrial radiation, therefore contributing to the increase in air temperature in the eastern part of Greater Cairo (Li et al., 2022), where the Mosque of Ahmad Ibn Tulun is located.

4. Conclusion

The present study investigated the trends in mean temperature for the selected World Heritage Sites in Egypt using the freely available, high-resolution WorldClim 2.1 gridded dataset for the period 1960–2021. Gridded data proved to be quite efficient for monitoring the changes in temperature patterns and could prove to be a proxy for further research. This study attempted to provide a general insight regarding the behavior of mean temperature at the selected World Heritage Sites in Egypt. It can be concluded from the empirical results that the mean temperature is increasing rapidly over the Sites located in lower Egypt and the Sinai Peninsula, and this also shows that there are multiple drivers that are contributing to the rise in mean temperature.

Monitoring the trends in temperature patterns for the selected World Heritage Sites helped in assessing the present status of these Sites in the context of a larger thermal picture of the region. This assessment and understanding can contribute to more site-specific research, taking into account more climatic parameters like rainfall, humidity, and so on, and also finding out how the World Heritage Site is responding to climate change, which eventually can help in formulating site-specific mitigation plans.

This study was limited to seven World Heritage Sites in Egypt. The seven World Heritage properties of Egypt consist of 23 locations, as some properties are associated with multiple Sites. This study involved selecting a single location from each World Heritage property, and this was done because Sites such as those of Nubian monuments, from Abu Simbel to Philae, consist of ten locations that are dispersed all over Aswan Governorate, and this necessitates a proper study focusing only on the Nubian monuments. Some World Heritage properties, like Ancient Thebes and its Necropolis, Memphis and its Necropolis, and Historic Cairo, have multiple locations but are not separated by long distances; therefore, no temperature variation was observed.

5. References

- Adams, J., & Faure, H. (1997). Review and Atlas of Palaeovegetation: Preliminary Land Ecosystem Maps of the World since the Last Glacial Maximum. https://www.esd.ornl.gov/projects/qen/new_africa.html
- Agbo, E., & Ekpo, C. (2021). Trend analysis of the variations of ambient temperature using Mann-Kendall test and Sen's estimate in Calabar, southern Nigeria. *Journal of Physics: Conference Series*, 1734(1), 012016.
- Becherini, F., Cassar, J., Galea, M., & Bernardi, A. (2016). Evaluation of the shelters over the prehistoric Megalithic Temples of Malta: Environmental considerations. *Environmental Earth Sciences*, 75, 1–13.
- Berkeley Earth. (2023). Berkeley Earth. <https://berkeleyearth.org/>
- Blavier, C. L. S., Huerto-Cardenas, H. E., Aste, N., Del Pero, C., Leonforte, F., & Della Torre, S. (2023). Adaptive measures for preserving heritage buildings in the face of climate change: A review. *Building and Environment*, 110832.
- Brimblecombe, P., Grossi, C. M., & Harris, I. (2011). Climate change critical to cultural heritage. *Survival and Sustainability: Environmental Concerns in the 21st Century*, 195–205.
- Camuffo, D. (1986). Deterioration processes of historical monuments. In *Studies in Environmental Science* (Vol. 30, pp. 189–221). Elsevier.
- Cave, C. (2022). Climate Change and World Heritage: An Introduction. *50 Years World Heritage Convention: Shared Responsibility–Conflict & Reconciliation*, 215–225.
- Chervenkov, H., & Slavov, K. (2019). Theil-Sen estimator vs. Ordinary least squares-trend analysis for selected ETCCDI climate indices. *Comptes Rendus Acad. Bulg. Sci*, 72, 47–54.
- Curiac, C.-D., & Micea, M. (2022). Evaluating Research Trends Using Key Term Occurrences and Multivariate Mann-Kendall Test. *2022 International Symposium on Electronics and Telecommunications (ISETC)*, 1–4.
- Domroes, M., & El-Tantawi, A. (2005). Recent temporal and spatial temperature changes in Egypt. *International Journal of Climatology*, 25, 51–63. <https://doi.org/10.1002/joc.1114>
- Elfadaly, A., Abouarab, M. A., Eldein, A. S., & Lasaponara, R. (2023). Remote Sensing Applications for Cultural Heritage Sites Sustainability: Case Studies from Egypt. In *Sustainable Conservation of UNESCO and Other Heritage Sites Through Proactive Geosciences* (pp. 615–639). Springer.
- Eid, M., Gad, E. H., & Abdel Basset, H. (2019). Temperature analysis over Egypt. *Al-Azhar Bulletin of Science*, 30(2-B), 13–30.
- Engelbrecht, F., Adegoke, J., Bopape, M.-J., Naidoo, M., Garland, R., Thatcher, M., McGregor, J., Katzfey, J., Werner, M., Ichoku, C., & others. (2015). Projections of rapidly rising surface temperatures over Africa under low mitigation. *Environmental Research Letters*, 10(8), 085004.
- Farouk, M. A. (2019, December 20). Egypt's "history of humanity" monuments face climate change threat. U.S. <https://www.reuters.com/article/us-egypt-climate-change-culture-trfn-idUSKBN1Y0OQE>
- Fick, S. E., & Hijmans, R. J. (2017). WorldClim 2: New 1-km spatial resolution climate surfaces for global land areas. *International Journal of Climatology*, 37(12), 4302–4315.
- Gocic, M., & Trajkovic, S. (2013). Analysis of changes in meteorological variables using Mann-Kendall and Sen's slope estimator statistical tests in Serbia. *Global and Planetary Change*, 100, 172–182.
- Harris, I., Osborn, T. J., Jones, P., & Lister, D. (2020). Version 4 of the CRU TS monthly high-resolution gridded multivariate climate dataset. *Scientific Data*, 7(1), 109. <https://doi.org/10.1038/s41597-020-0453-3>
- Haylock, M., Hofstra, N., Klein Tank, A., Klok, E., Jones, P., & New, M. (2008). A European daily high-resolution gridded data set of surface temperature and precipitation for 1950–2006. *Journal of Geophysical Research: Atmospheres*, 113(D20).
- Hereher, M. E. (2016). Time series trends of land surface temperatures in Egypt: A signal for global warming. *Environmental Earth Sciences*, 75, 1–11.
- Ismael, H. (2015). The climate and its impacts on Egyptian civilized Heritage: Ei-Nadura temple in El-Kharga oasis, western desert of Egypt as a case study. *Present Environment and Sustainable Development*, 1, 5–32.
- Jain, L., & Bhatt, B. (2022). A spatio-temporal analysis of changing trends in rainfall patter: A case study of Kutch District. *Journal of Geomatics*, 16(2), 223–235.
- James J. MacCarthy, O.F Canziani, N.A Leary, D.J Dokken, & K.S White. (2001). *Climate Change 2001: Impacts, Adaptation, and Vulnerability Report of IPCC Working Group II*. <https://archive.ipcc.ch/ipccreports/tar/wg2/index.php?idp=144>
- Jiqin, H., Gelata, F. T., & Chaka Gameda, S. (2023). Application of MK trend and test of Sen's slope

- estimator to measure impact of climate change on the adoption of conservation agriculture in Ethiopia. *Journal of Water and Climate Change*, 14(3), 977–988.
- Kandya, A., Sarkar, J., Chhabra, A., Chauhan, S., Khatri, D., Vaghela, A., & Kolte, S. (2021). Statistical Assessment of the Changing Climate of Vadodara City, India During 1969-2006. *European Journal of Climate Change*, 3, 1–18. <https://doi.org/10.34154/2021-EJCC-0015-01-18/eurass>
- Khatib, A. N. (2023). Climate change and travel: Harmonizing to abate impact. *Current Infectious Disease Reports*, 25(4), 77–85.
- Lee, H., Calvin, K., Dasgupta, D., Krinner, G., Mukherji, A., Thorne, P., Trisos, C., Romero, J., Aldunce, P., Barrett, K., & others. (2023). Climate Change 2023: Synthesis Report. Contribution of Working Groups I, II and III to the Sixth Assessment Report of the Intergovernmental Panel on Climate Change. The Australian National University.
- Li, X., Stringer, L. C., & Dallimer, M. (2022). The impacts of urbanisation and climate change on the urban thermal environment in Africa. *Climate*, 10(11), 164.
- Mahmoud, H. F. (2019). Parametric versus semi and nonparametric regression models. *ArXiv Preprint ArXiv:1906.10221*.
- Malakouti, S. M. (2023). Utilizing time series data from 1961 to 2019 recorded around the world and machine learning to create a Global Temperature Change Prediction Model. *Case Studies in Chemical and Environmental Engineering*, 7, 100312.
- Masson-Delmotte, V., Zhai, P., Pörtner, H., Roberts, D., Skea, J., Shukla, P., Pirani, A., Moufouma-Okia, W., Péan, C., & Pidcock, R. (2018). IPCC Special Report on Impacts of Global Warming of 1.5 C above Pre-industrial Levels in Context of Strengthening Response to Climate Change. In *Sustainable Development, and Efforts to Eradicate Poverty*.
- Mohammad, L., Mondal, I., Bandyopadhyay, J., Pham, Q. B., Nguyen, X. C., Dinh, C. D., & Al-Quraishi, A. M. F. (2022). Assessment of spatio-temporal trends of satellite-based aerosol optical depth using Mann-Kendall test and Sen's slope estimator model. *Geomatics, Natural Hazards and Risk*, 13(1), 1270–1298.
- Newsome, D., Dowling, R., & Leung, Y.-F. (2012). The nature and management of geotourism: A case study of two established iconic geotourism destinations. *Tourism Management Perspectives*, 2, 19–27.
- NOAA. (2019, February). National Oceanic and Atmospheric Administration. Climate Data Monitoring | National Oceanic and Atmospheric Administration. <https://www.noaa.gov/education/resource-collections/climate/climate-data-monitoring>
- Pörtner, H. O., Roberts, D. C., Adams, H., Adler, C., Aldunce, P., Ali, E., Begum, R. A., Betts, R., Kerr, R. B., Biesbroek, R., & others. (2022). Climate change 2022: Impacts, adaptation and vulnerability. IPCC.
- Rahman, G., Rahman, A., Anwar, M. M., Dawood, M., & Miandad, M. (2022). Spatio-temporal analysis of climatic variability, trend detection, and drought assessment in Khyber Pakhtunkhwa, Pakistan. *Arabian Journal of Geosciences*, 15(1), 81.
- Raju, G. (2021). Assessment of impact vulnerability and farm households adaptation to climate change a study of Telangana [PhD Thesis, University of Hyderabad]. <http://hdl.handle.net/10603/419242>
- Rezvi, H. U. A., Tahjib-Ul-Arif, M., Azim, M. A., Tumpa, T. A., Tipu, M. M. H., Najnine, F., Dawood, M. F., Skalicky, M., & Brestič, M. (2023). Rice and food security: Climate change implications and the future prospects for nutritional security. *Food and Energy Security*, 12(1), e430.
- Sabbioni, C., Brimblecombe, P., & Cassar, M. (2010). The atlas of climate change impact on European cultural heritage: Scientific analysis and management strategies. Anthem Press.
- Sabbioni, C., Cassar, M., Brimblecombe, P., & Lefevre, R.-A. (2008). Vulnerability of cultural heritage to climate change. *European and Mediterranean Major Hazards Agreement (EUR-OPA)*, 1–24.
- Sardella, A., Palazzi, E., von Hardenberg, J., Del Grande, C., De Nuntis, P., Sabbioni, C., & Bonazza, A. (2020). Risk mapping for the sustainable protection of cultural heritage in extreme changing environments. *Atmosphere*, 11(7), 700.
- Sesana, E., Gagnon, A. S., Ciantelli, C., Cassar, J., & Hughes, J. J. (2021). Climate change impacts on cultural heritage: A literature review. *Wiley Interdisciplinary Reviews: Climate Change*, 12(4), e710.
- Sitzia, F., Lisci, C., & Mirão, J. (2021). Accelerate ageing on building stone materials by simulating daily, seasonal thermo-hygrometric conditions and solar radiation of Csa Mediterranean climate. *Construction and Building Materials*, 266, 121009. <https://doi.org/10.1016/j.conbuildmat.2020.121009>

- Thenmozhi, M., & Kottiswaran, S. (2016). Analysis of rainfall trend using Mann-Kendall test and the Sen's slope estimator in Udumalpet of Tirupur district in Tamil Nadu. *International Journal of Agricultural Science and Research*, 6(2), 131–138.
- Vyshkvarkova, E., & Sukhonos, O. (2023). Climate Change Impact on the Cultural Heritage Sites in the European Part of Russia over the past 60 Years. *Climate*, 11(3), 50.
- Yue, S., & Wang, C. Y. (2002). Applicability of prewhitening to eliminate the influence of serial correlation on the Mann-Kendall test. *Water Resources Research*, 38(6), 4–1.